ELSEVIER

Physica D 103 (1997) 505–527

PHYSICA D

Coupled maps with growth and death: An approach to cell differentiation

Kunihiko Kaneko

Department of Pure and Applied Sciences, University of Tokyo, Komaba, Meguro-ku, Tokyo 153, Japan

Abstract

An extension of coupled maps is given which allows for the growth of the number of elements, and is inspired by the cell differentiation problem. The growth of elements is made possible first by clustering the phases, and then by differentiating roles. The former leads to the time sharing of resources, while the latter leads to the separation of roles for the growth. The mechanism of the differentiation of elements is studied. An extension to a model with several internal phase variables is given, which shows differentiation of internal states. The relevance of interacting dynamics with internal states ("intra–inter" dynamics) to biological problems is discussed with an emphasis on heterogeneity by clustering, macroscopic robustness by partial synchronization and recursivity with the selection of initial conditions and digitalization.

1. Introduction

Coupled map lattices (CML) have been used to study many diverse phenomena of spatially extended systems [1]: (i) spatio-temporal chaos, (ii) statistical mechanics of an ensemble of chaotic elements, (iii) turbulence, (iv) pattern dynamics, (v) neural dynamics and applications to information processing, and (vi) biological network problems.

Although the CML approach has been developed rapidly in the first four fields [2] and partly in the neural information processing field, it has not been developed so much in applications to biological networks.

One of the important merits in applying CML techniques to biological networks lies in the ability to capture the interplay between inter-unit and intra-unit dynamics. Such "intra–inter dynamics" seems to be essential to a variety of biological problems. In cell biology, there are complex metabolic reaction dynamics in each unit (cell), which are affected by the interaction among cells. In neural systems, the viewpoint of intra–inter dynamics must be essential to the formation of internal images. An ecological system also consists of interacting units with internal dynamics. A CML gives a simple model for a system composed of interacting units with internal dynamics, and thus fits with biological problems better than a cellular automaton, where there is no internal dynamics in each element.

Indeed, there have been some studies for cellular biology adopting this dynamical systems approach.

The importance of temporal oscillations in cellular dynamics was studied in pioneering work by Goodwin [3]. Recently, the existence of oscillatory dynamics for cell division processes has been discussed both experimentally and theoretically in cycline and M-phase-promoting factor [4]. On the other hand, different cell types are attributed to the coexistence of many attractors by Kauffman [5] where a Boolean network is adopted for each cellular dynamics. Starting from such internal cellular dynamics, cell-to-cell interactions are included to study the Turing-type pattern formation

PII S0167-2789(96)00282-5

mechanism [6]: Attraction to different states is found in a coupled system of Boolean-network-type differential equations [7], while a CML corresponding to Goodwin-type oscillators is studied by Bignone [8].

As for the interactions, these studies basically adopt the pattern-formation mechanism of the Turing instability [6]. The internal dynamics is based either on stable cycles, or on switching-type threshold dynamics allowing only for fixed points. Use of chaos or transient unstable dynamics has not been discussed. Another missing factor in these studies is the change in degrees of freedom by cell division and death, while selection of the system size and boundary condition through the dynamics itself is one important characteristic feature in a biological system. These are few of several motivations to introduce the isologous diversification to be discussed in Section 2. With the theory we try to answer the questions of the mechanism of the differentiation process in conjunction with the growth in cell numbers, and how cellular memory is formed that is transferred stably through cell divisions.

In general, there is an important missing factor in applying the CML approach to study a biological problem. Indeed, this drawback is common in the dynamical systems (DS) approach to modeling, which may be termed the "separation" problem. A model constructed using the DS approach consists of time, a set of states, an evolution rule, an initial condition of the states, and boundary conditions. It is generally assumed that these four sets themselves are separated from each other: Although the states are changed according to the evolution rule, the set of states itself (e.g., the number of variables) is fixed independent of the rule. The states cannot change the evolution rule itself. Initial conditions and boundary conditions are chosen independently of the state values and of the evolution rule. In biological problems, such separation between all these elements of the model may not be valid, or at the very least the origin of their separation should be discussed.

Let us first discuss the separation between the set of states and the evolution rule. In a biological system, the evolution rule itself is formed and changes in connection with the temporal evolution of the states. A simple example is the change of the number of variables itself with time: Let us consider the dynamics of a cell society. When one considers the chemical variability of cells, we need a set of variables for each cell. Then, the number of variables should change with the cell division and death. Or, consider another example: population dynamics. There the emergence of new species leads to a change in the degrees of freedom. Such growth of elements is also seen in economics, where the number of agents can change in time through reproduction and extinction.

Another aspect of the separation problem lies in the segregation of parameters and variables. In dynamical systems, the roles of "parameters" and "variables" are predetermined and fixed. In a biological system such separation may not be possible, or rather, it is important to discuss how some sets of variables turn into parameters.

The next important problem lies in the choice of initial conditions or boundary conditions. For a cell to grow repeatedly, the initial condition of its internal state should satisfy some condition. This initial condition, however, is determined by its mother cell's state. Thus, the initial conditions of a state, and its evolution are not clearly separated. Through the evolution of the state, initial conditions are selected that allow for recursive growth.

Recently, the author and Yomo have proposed a novel scenario for cell differentiation termed "*isologous diversification theory*" [9]. The cell differentiation and developmental processes involve internal metabolic reactions, which are nonlinear, as well as cell division and death, which lead to change of the degrees of freedom of the system. Thus, the study of cell differentiation is one prototype of our intra–inter dynamics picture for biological systems.

The present paper is organized as follows. In Sectioin 2 we explain the isologous diversification theory in terms of a coupled metabolic reaction model. In Sections 3 and 4, we study a minimal model of the differentiation process, given by a globally coupled circle map which allows for a change in the number of elements (cells). Cells divide or die according to the history of the rotation of their phase. We also elucidate the mechanism by which the phases of oscillation, as well as their growth rates are differentiated.

In Section 5, we extend the model to include several phase variables and see how differentiation of elements is embedded into the internal dynamics. The paper concludes in Section 6 with a discussion of our results.

2. Isologous diversification for cell differentiation

The author and Yomo have studied a class of intra–inter dynamical models which are a dynamic model for the cell differentiation process [9–11]. This class of models consists of a metabolic or genetic network within each cell, and interaction between cells through competition for nutrition and the diffusion flow of chemicals to media. In each cell there is a set of chemical variables. When a cell is isolated, its chemicals are assumed to show oscillatory behaviors of a Lotka–Volterra type, that is, the concentration of each chemical component switches between a low and high level periodically in time. As for the inter-dynamics, cells are assumed to interact with each other through the media. The interaction here is global, and the system belongs to a class of globally coupled dynamical systems. The cell is assumed to divide and thus gives birth to a new cell when a product of the metabolic chemical reactions exceeds some threshold. The concentrations of chemicals of two divided cells are chosen to be almost identical upon the division.

Starting from a single cell initial condition, we have found the following scenario for cell growth and differentiation.

(1) *Synchronous oscillations of identical cells:* Up to some threshold number of cells, all oscillate synchronously, and their states are identical.

(2) *Differentiation of the phases of oscillations of internal states:* When the number of cells exceeds the threshold, they lose identical and coherent dynamics. The phases of oscillations split into several groups (clusters). This clustering is a general consequence of coupled oscillators (maps) [12–15], when there is strong interaction among them (similar clusterings are also found in a system without local but with collective chaos [16]).

(3) *Differentiation of the amplitudes of internal states:* At this stage, the states of cells are different even after taking the temporal average over periods. The pattern of orbits in the chemical phase space differs by groups. The dynamics as well as the average behavior of cells is differentiated.

(4) *Transfer of the differentiated state to their offsprings by reproduction:* The differentiated character of a cell is transferred to its offsprings. This "memory" is made possible through the transfer of initial conditions for the chemical variables of the reproduced new cell.

As the cells continue to reproduce, the competitive interaction among them gets stronger and leads to successive diversification of their behavior. Generally speaking, identical elements tend to become diversified through the interplay of nonlinear oscillations, cell-to-cell interaction, and reproduction. The first three stages listed above are consequences of globally coupled dynamical systems. The emergence of the fourth stage, on the other hand, is attained only through the reproduction of cells, where the initial conditions are selected so that the offsprings keep the same character as their mother cell. We believe that this emergence of recursivity or memory is an important feature of coupled dynamical systems with reproduction, and thus is essential to the information flow and memory in biological systems.

Of course, the idea to attribute a different cell type to a different state of chemical dynamics is not new. As mentioned in Section 1, the existence of multiple fixed point states in Boolean networks has been proposed to provide different cell types [5], while different oscillatory states coexist with the inclusion of cellular interactions [7,8]. In comparison with these previous dynamical-systems models for cell differentiation, however, the proposal of our theory is novel as to the following points:

(i) *Importance of instability*: In the second stage, clustering by coupled nonlinear oscillators is essential to the trigger of differentiation. For the clustering, the orbital instability of a system is required, either by internal dynamics or through interactions. The dynamics of the attractor itself

is not necessarily chaotic, but an instability at least during transient time steps is required.

(ii) *Non-diffusive interaction*: In contrast with the previous theoretical models for differentiation, the interaction form is not diffusive as postulated for the Turing instability, but is based on the (global) competition for chemical resources. With this interaction, differentiation proceeds. In particular, this form seems to be essential to the fixation of differentiation (with amplitude clustering) at the third stage.

(iii) *Stability at an ensemble level*: Our differentiation is based on the interaction among nonlinear elements. In such a coupled system, stability of a collective dynamics has been studied, that is formed by an ensemble of chaotic elements [12,17,18]. Such stability is essential to our scenario, and is indeed found in our simulations [10]. For example, when all cells of some type are removed, other cells of a different type are transformed into the removed type, through divisions. With these changes of cell types, the cellular distribution comes back to the original one. This stability is especially important for the maintenance of a biological system.

(iv) *Change of degrees of freedom in conjunction with dynamics*: Cell division and death lead to the change in degrees of freedom, which provides a novel class of dynamical systems. There a novel type of instability is proposed as "open chaos" [19] where the orbital instability in global phase space is in conjunction with the change of degrees of freedom. Another important factor in such a system is the selection of system size. With cell division and death, the variation of the total number of cells remains within some range. Such autonomous selection of the system size is important in a biological system. For example, apoptosis is essential to the selection of the total number of cells in a system, and our model may give a conceptual model of it.

(v) *Recursive transmission through selection of initial conditions*: The cellular memory at the fourth stage is formed as the result of the selection of initial conditions for a cellular state (i.e., a partial system of the total dynamical system). This argument is possible only for a system with a cell division process, internal dynamics, and interactions. As for the choice of initial conditions of the internal cellular system, this selection could be related with the basin for multiple attractors. However, in our model, the cellular interactions are also relevant to the formation of multiple cellular states and the selection of one of them. The coexistence of multiple states and the selection are also the outcome of both the interactions and internal dynamics.

3. Coupled map model with division and death: Relation with growth and synchronization

The cell differentiation model adopted in [9,11] is rather complicated in order to correspond with biochemical reactions. In this section we consider a very simple, possibly the simplest, model with internal oscillatory dynamics, competitive interaction, and growth in the degrees of freedom.

First we assume that there is a variable, $x(i)$, determining the cell state, and that cells compete with each other for a source term s. The source is supplied from the outer environment with a constant rate s. The ability to get this source depends on the internal state $x(i)$. Thus the dynamics of each $x(i)$ is given by

$$x_{n+1}(i) = x_n(i) + f(x_n(i)) + S_n, \tag{1}$$

$$S_n = \frac{s - \sum_j f(x_n(j))}{N}. \tag{2}$$

The term $x_{n+1}(i) - x_n(i) = f(x_n(i)) + S_n$ gives a source term that the element i takes at the time step n. The second condition assures $\sum_i \{x_{n+1}(i) - x_n(i)\} = s$, that is, the sum of the source term balances with that supplied externally. The summation is over the number of elements N.

Since $x_n(i)$ represents an internal state, which is oscillatory, it is natural to relate it with the phase of oscillation. This correspondence inspires us to choose the periodic function of $f(x) = (K/2\pi)\sin(2\pi x)$, so that the dynamics depends only on the phase, represented by the fractional part of $x(i)$. It is useful

then, to relate the threshold for division with the number of cycles after the previous division. Hence we assume that the condition for division and death is governed by the the number of oscillations, given by the integer part of $x_n(i)$. Taking these considerations into account, we choose the following rules for the division and death:

(A) Divide cell i if $x_n(i) > T_g$. After division, $x_n(i)$ of cell i and the new element $N+1$ is assigned to be $\frac{1}{2}(x_n(i) - T_g) + \delta$ and $\frac{1}{2}(x_n(i) - T_g) - \delta$, respectively, with δ a very small random number.

(B) Remove cell i if $x_n(i) < T_d$.

Here $T_g \geq 1$ and $T_d \leq 0$ are integers giving the threshold for growth (division) and death, respectively. We often call element i as cell i, and the duration from its birth (or division) to the next division (or death) as the cell's lifecycle, following the analogy with cell biology. The number of time steps from its latest division (or birth) to the next division (or death) is called its lifetime. Although no difference exists besides the error term between the two cells i and $N+1$, produced by the division of the cell i, one of them remains to be called cell i. Since each cell i can divide several times, we attribute a lifecycle and lifetime to each division process, here. (Thus there can be several lifetimes for cell i according to successive divisions).

The model of (1) is a globally coupled map (GCM) with the coupling term given by (2). Thus it is expected that the dynamics of (1) leads to the clusters of synchronized oscillations as in globally coupled circle maps [13], which are relevant to the dynamics of growth. Here a cluster is defined as a set of elements having identical fractional parts of $x(i)$ up to a prescribed precision. The integer part of $x_n(i)$ is not taken into account for the definition of clustering, since the dynamics (1) only depends on the fractional part, and two elements with the same fractional part show identical oscillations until the division occurs to which the integer part is relevant. In other words, the dynamics of the phase variable $x(i)$ is identical up to this precision for elements belonging to an identical cluster. If all elements belong to a single cluster, they are synchronized perfectly. Since the integer part of $x_n(i)$ can be different even for two cells belonging to the same cluster, the division condition can be applied to them at different time steps. (Note that the history of two elements (such as the time of the latest division) can be different even if two elements are synchronized at the moment). Through this division process, two completely synchronized elements (even up to an infinite precision) can change their values. Thus the clustering condition itself is dynamic, in contrast with the clustering of an attractor in GCM [12].

In the present paper we define a cluster at each time step with a precision of 10^{-5}. A state of an ensemble of cells is classified by the number of synchronized clusters k and the number of elements for each cluster N_k, i.e., the partition of N elements to k clusters as $(N_1, N_2, \ldots, N_k)$.

Here we mainly discuss the simulations with $T_d = 0$. In this case, the number of cells does not grow indefinitely. As K is increased, we have seen roughly three phases: [1]

(1) Ordered phase.
(2) Partially ordered phase.
(3) Desynchronized phase.

Each phase is characterized as follows (see Fig. 1 for the time series of $x_n(i)$ for each phase):

(1) Elements tend to be synchronized: As shown in the time series (see Fig. 1(a)), elements' oscillations split into two clusters for some interval, and then all of them tend to be synchronized, and later split into two (or a few) clusters. This process repeats with time as $x_n(i)$ increases, within each cell's lifecycle. As the number of cells increases, their oscillations increase the mutual coherence, in the present model. When the number gets larger, all cells' oscillations become coherent. Then there appears simultaneous death of multiple cells, and the number of cells decreases drastically, from which the growth again starts (see Fig. 2(a) for the change of the total number of cells N). Thus the system has two levels of cycles; one is the intra-cellular oscillation, and the other the inter-cellular oscillation associated with the change of the number of cells.

[1] see [20] for the discovery of these phases for $T_g = 1$.

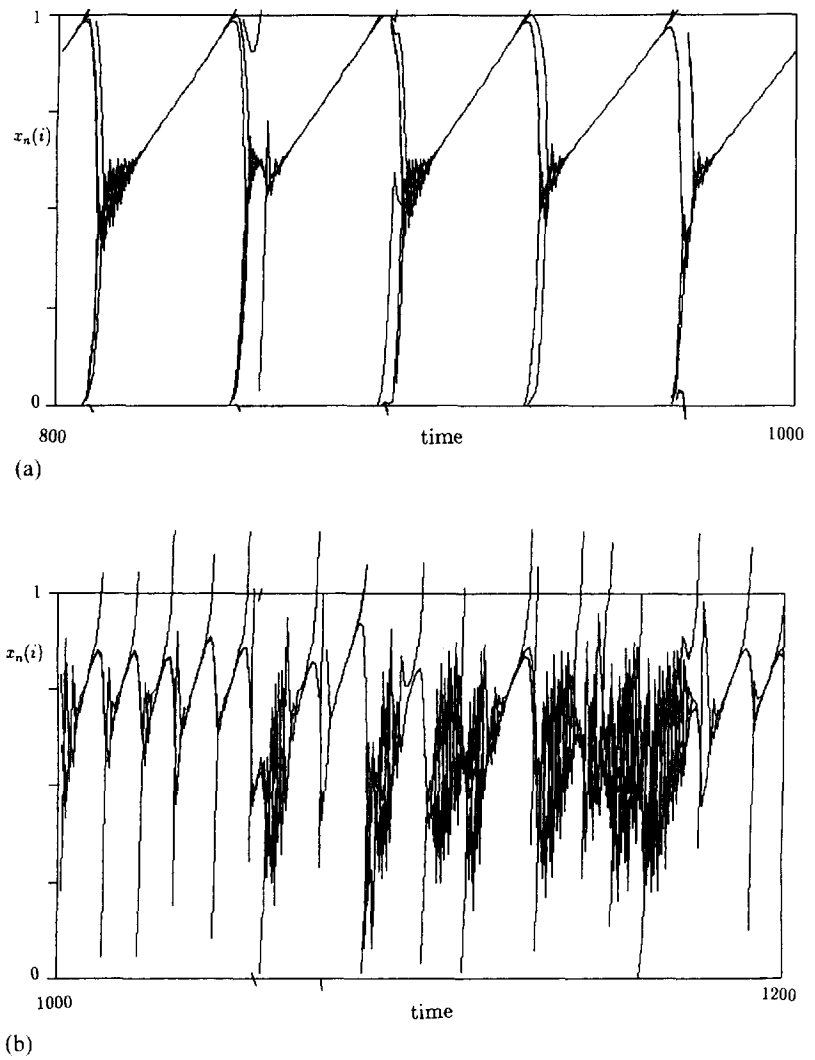

Fig. 1. Continued

(2) Partially ordered phase: Around $K \approx 3.3$ the oscillations of identical cells can be desynchronized. The cluster number fluctuates between 1 and N, while the coupled system consists of a single large synchronized cluster (i.e., $N_1 \sim \frac{1}{2}N$) and many other desynchronized elements. Here the number of cells can grow up to a very large number. Indeed, as is seen in Fig. 2(c), there are two temporal regimes; for most of the time the number oscillates around O(10), but occasionally there appears an intermittent burst to a very large number of cells (100–700). The time series in the former regime is given in Fig. 1(b), while that for the latter case is given in Fig. 1(c). In this partially ordered phase, the number of cells often stays at a large value for about a million steps, until there is a simultaneous death of many cells. After the death of many cells, new cells start growing as in Fig. 1(d). Detailed study of this phase is given in Section 4.

(3) Desynchronized states: For $K > 3.4$, elements' oscillations are typically desynchronized. For most time steps, all elements are desynchronized with each other, i.e., the cluster number is N (see

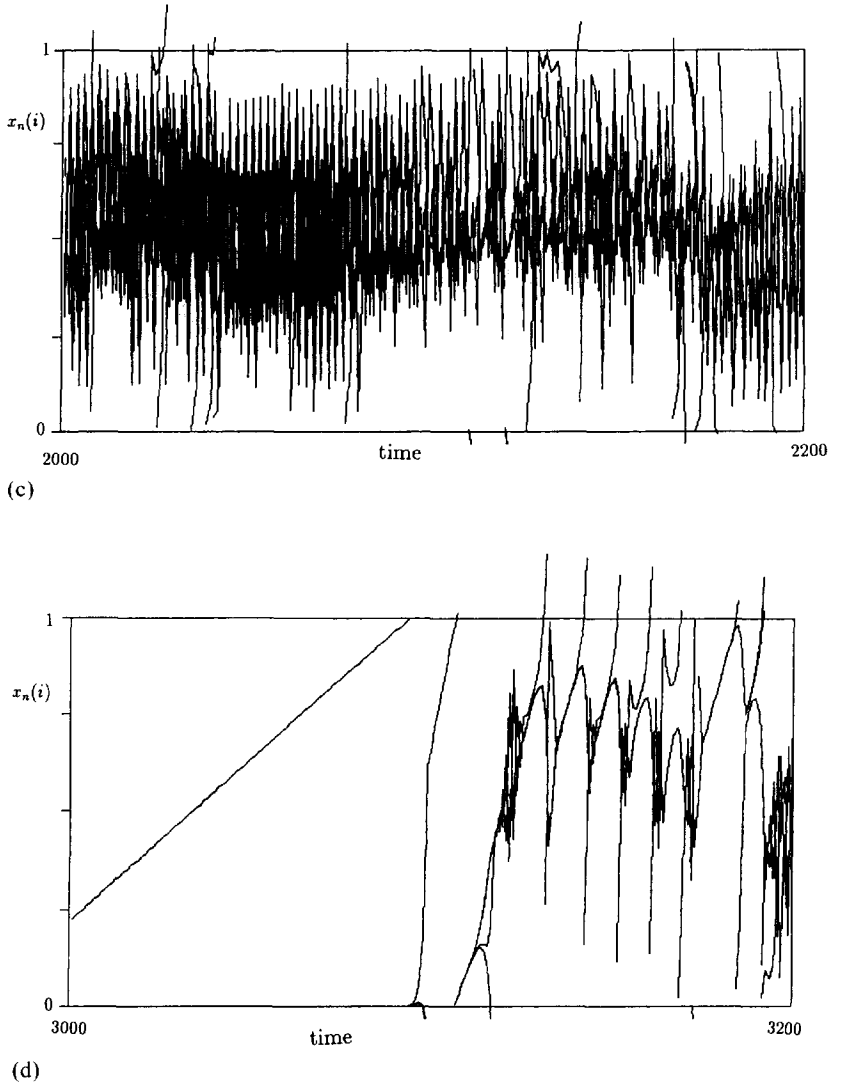

Fig. 1. Continued

Fig. 1(e), where the number of cells fluctuates between 2 and 6). Growth of the number of cells is suppressed. The number fluctuates at a low level, with an irregular oscillation.

To see the above changes quantitatively, the maximal and average numbers of cells are plotted as a function of K in Fig. 3. There is a sharp peak at $K \approx$ (3.2–3.3), independent of the choice of threshold T_g. At $3 < K < 3.4$, the maximal cell number is over a thousand (see Fig. 1), which is due to the existence of a temporal regime allowing for a steady increase to a large number and its maintenance (see Fig. 2(c)). In Fig. 4 we have also plotted the average fraction of cluster numbers, i.e., $\langle k \rangle / \langle N \rangle$, where $\langle\ \rangle$ is the temporal average. There is a sharp increase at $K \approx 3.3$, beyond which the fraction is close to 1, meaning complete desynchronization.

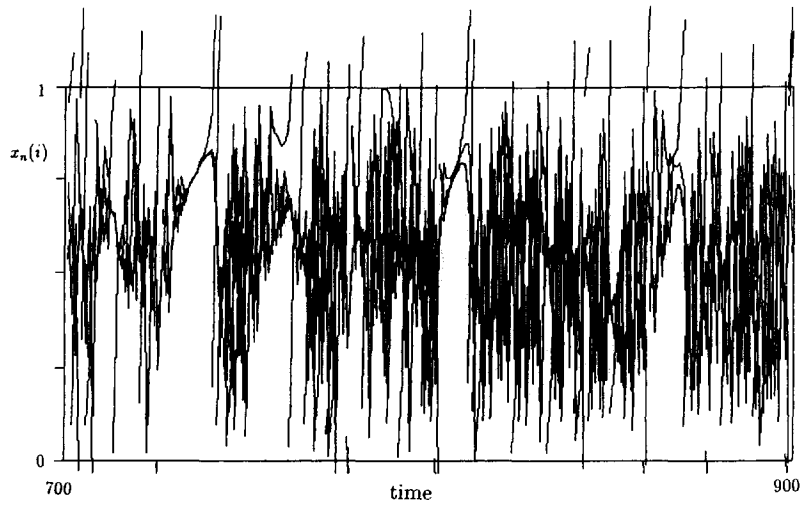

(e)

Fig. 1. The overlaid time series of the fractional part of $x_n(i)$. When $x_n(i)$ exceeds 1, the line continues from $x_n(i) - \mathrm{Int}(x_n(i))$, with $\mathrm{Int}(z)$ as the integer part of z. The number of lines changes with division and death. $T_g = 10$, $T_d = 0$, $s = 0.1$. (a) $K = 2.0$ (b)–(d) $K = 3.3$ (e) $K = 4.0$.

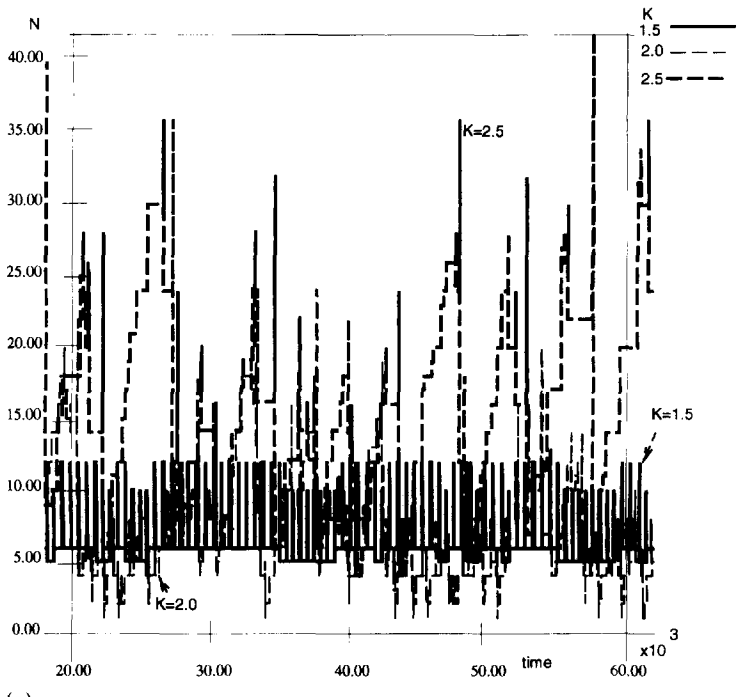

(a)

Fig. 2. Continued

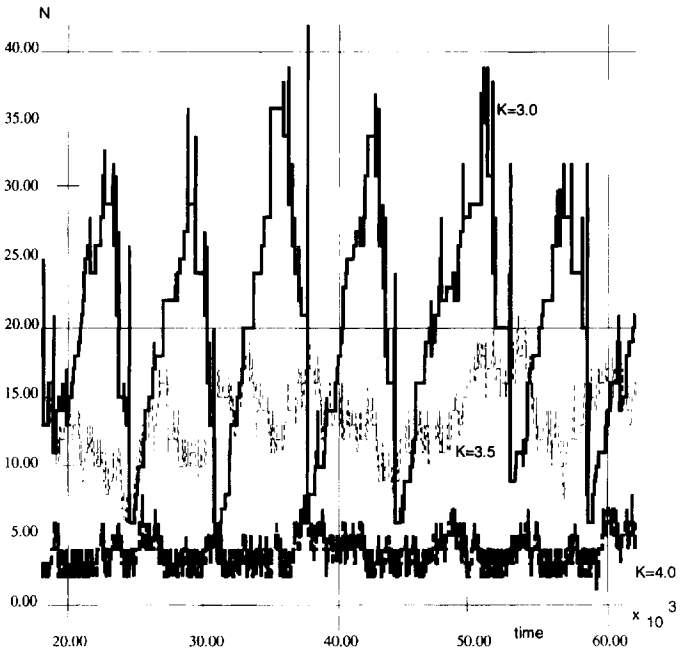

(b)

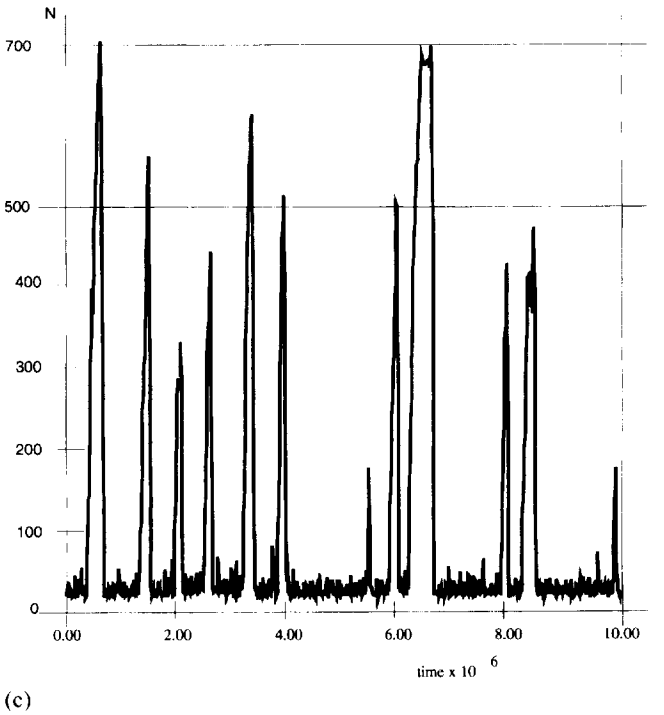

(c)

Fig. 2. Temporal evolution of the number of cells N. $T_g = 10$, $T_d = 0$, $s = 0.1$ for (a) $K = 1.5$, 2.0, 2.5, (b) $K = 3.0$, 3.5, 4.0 and (c) $K = 3.3$.

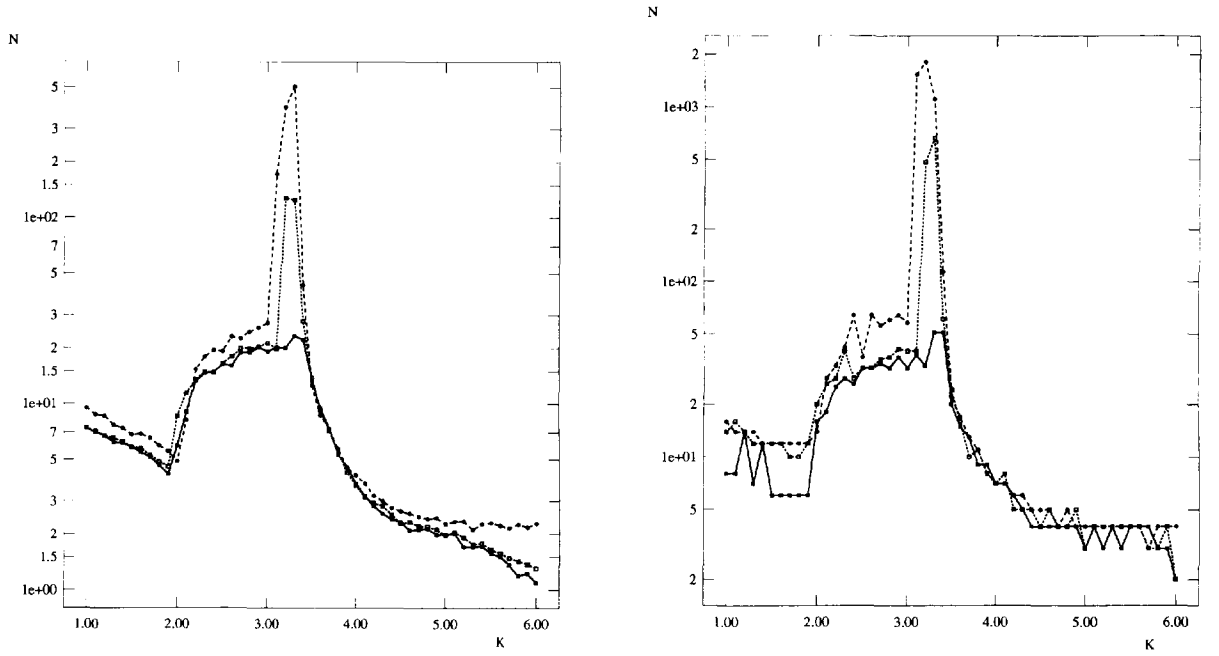

Fig. 3. The average (a) and maximal number (b) of cells over the time steps 5000–105 000. Simulations are carried out with $s = 0.1$, $T_d = 0$, and starting from one cell. $T_g = 100$ (solid line with □), 10 (dotted line with □), and 1 (broken line with ○).

To see the instability of synchronization, it is useful to introduce the split exponent following the definition given in GCM [21]. It is defined as the rate of amplification of $x_n(i) - x_n(j)$ of two elements such that $x_n(i) \approx x_n(j)$. Since the global interaction term is common to all elements, the exponent is given by the average of the expansion rate for the one-body part of Eq. (1), i.e., $x_{n+1} = x_n(i) + f(x_n(i))$. Thus it is defined as

$$\lambda_{\mathrm{spl}}(i; T_0, T) = (1/T) \sum_{n=T_0}^{T_0+T} \log |1 + f'(x_n(i))|. \quad (3)$$

The above exponent is an average over time steps T_0 to $T_0 + T$. If the element remains existing forever, it is possible to take the infinite time limit to obtain a well-defined quantity like the Lyapunov exponent, as long as we do not take into account the perturbation caused by the "division process", which is not represented by the mapping process. In our problem cells can divide or die, where a threshold-type instability sets in. Still, the following quantifiers should be relevant to discuss the split instability: (a) The average of the exponent over all cells and over all time steps – this quantity, denoted as λ_{spl}, measures the average tendency of desynchronization. (b) The average of $\lambda_{\mathrm{spl}}(i; T_0, T)$ over a cell's lifecycle (i.e., from its latest division (or birth) to its next division (or death)) – this quantity is obtained just by taking T_0 as the latest first division time (or birth) and $T + T_0$ as the next division time (or death). The quantity measures an average degree of synchronization of a cell over its lifecycle.

The change of the average split exponent λ_{spl} versus K is given in Fig. 5. The exponent becomes positive around $K \approx 2$. We note that the growth of cell numbers starts to increase at $K > 2$. Between $2 < K < 2.9$, which corresponds to the ordered phase, the average exponent remains close to zero, as the "synchronization to few clusters" and "split by division" are balanced. This balance is shown in Fig. 1(a), where the above two processes repeat in each cell's oscillation within each lifecycle. For $K > 2.9$ the exponent

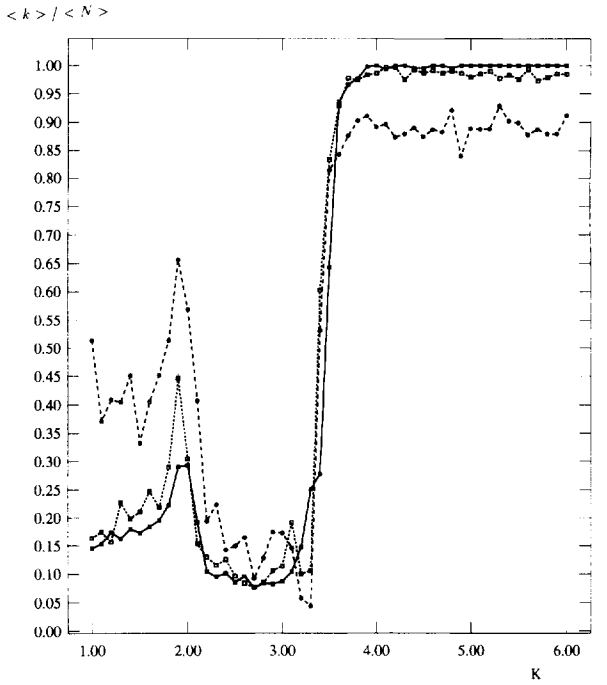

Fig. 4. Fraction of the average number of clusters to the total number of cells, i.e., $\langle k \rangle / \langle N \rangle$, obtained from the simulations for Fig. 3. $T_d = 0$, and $s = 0.1$. $T_g = 100$ (solid line with □), 10 (dotted line with □), and 1 (broken line with ○).

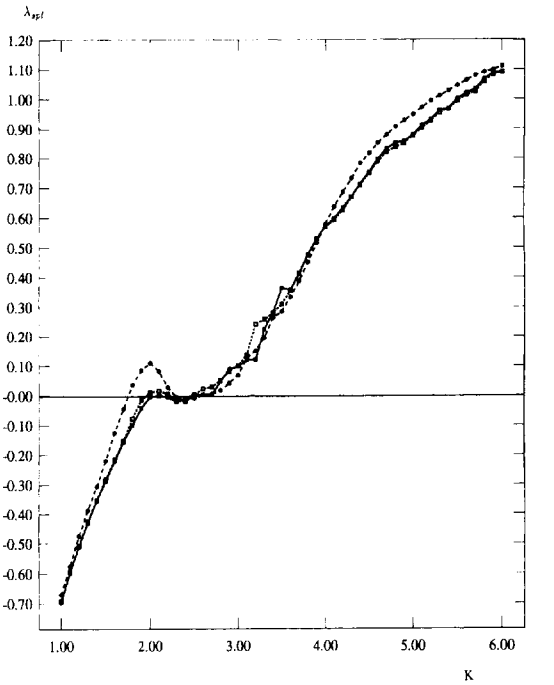

Fig. 5. Split exponent λ_{spl} plotted with the change of K, corresponding to Figs. 3 and 4. $T_g = 100$ (solid line), 10 (dotted line), and 1 (broken line).

starts to be positive, and increases slowly thereafter with K, until $K \approx 3.3$, where the increase starts to be larger. The regime $2.9 < K < 3.4$ corresponds to the partially ordered phase. For $K > 3.4$, i.e., at the desynchronized phase, the exponent smoothly increases with K.

The internal dynamics differs between cells that succeed in division, and those that will die. In Fig. 6, we have plotted the histogram of the split exponent over a cell's lifecycle for the cases of division and death, while the split exponent versus the cell's lifetime is given in Fig. 7. As in Fig. 7(b), most cell deaths occur within a few steps after a cell's latest division. Such "quickly" dying cells produce a peak in the histogram for $\lambda_{spl} > 1$ in Fig. 6(b), while those cells that died 10 steps after their latest division produce a peak around 0.3. Some dividing cells also produce a broad peak around 0.3, while those cells dividing after 100 000 steps lead to a different peak of the exponent, around 0.15, as shown in Figs. 6(a) and 7(a), respectively. In Fig. 7(a), we note that there are two groups of cells with differing split exponents. This implies that cells with long lifetimes are differentiated into two groups; one with very long lifetimes and the other with less long ones (but much longer than quickly dying cells).

Indeed such long-living cells appear while the number of cells is large as in Fig. 2(c). We will discuss the mechanism of this differentiation in Section 4.

As is seen in Fig. 3(a), the growth of cells is enhanced in the partially ordered phase where elements are partially synchronized. It should be noted that the maximum rate of growth occurs not at the marginal stability point ($\lambda \approx 0$), but in the regime with a small positive value, in contrast with the "edge of chaos"-type picture.

If the oscillations of all the elements are synchronized, then all elements compete for the source term at the same time. This intense competition does not allow for an effective use of resources. Instead, through the

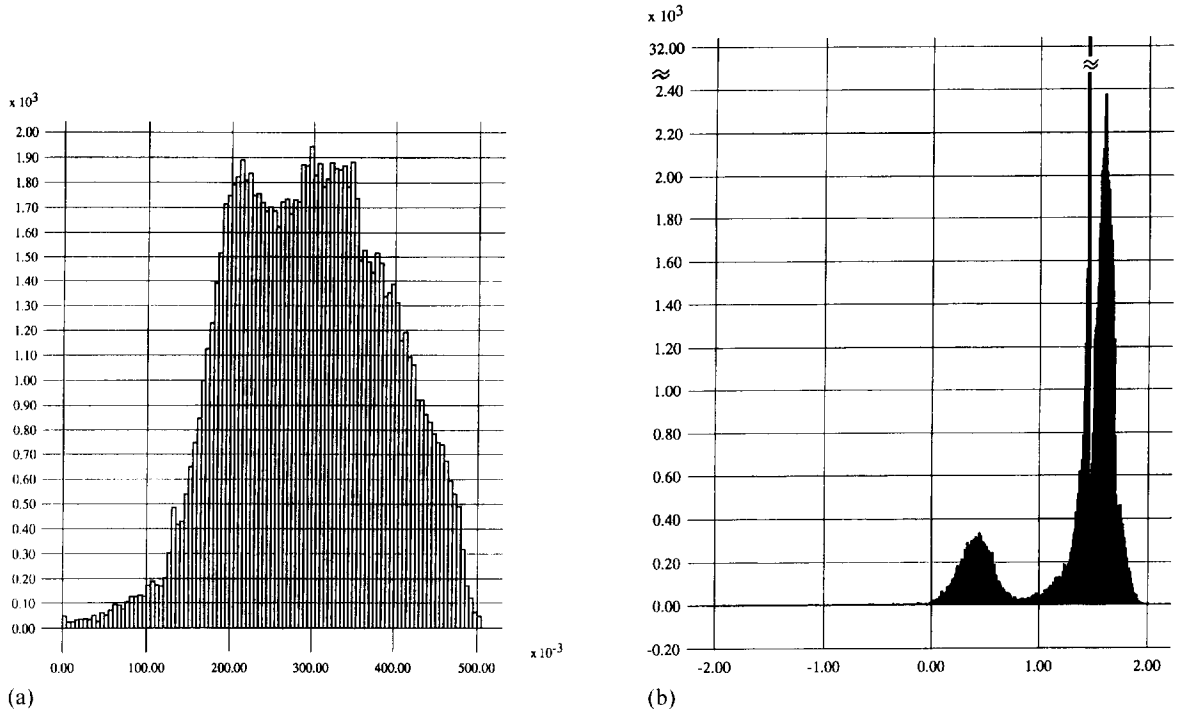

Fig. 6. Histogram of the split exponent over a cell's lifecycle. $K = 3.3$, $s = 0.1$, $T_g = 10$, and $T_d = 0$ (a) for cells that divide successfully after their lifecycle, and (b) for cells that die after their lifecycle.

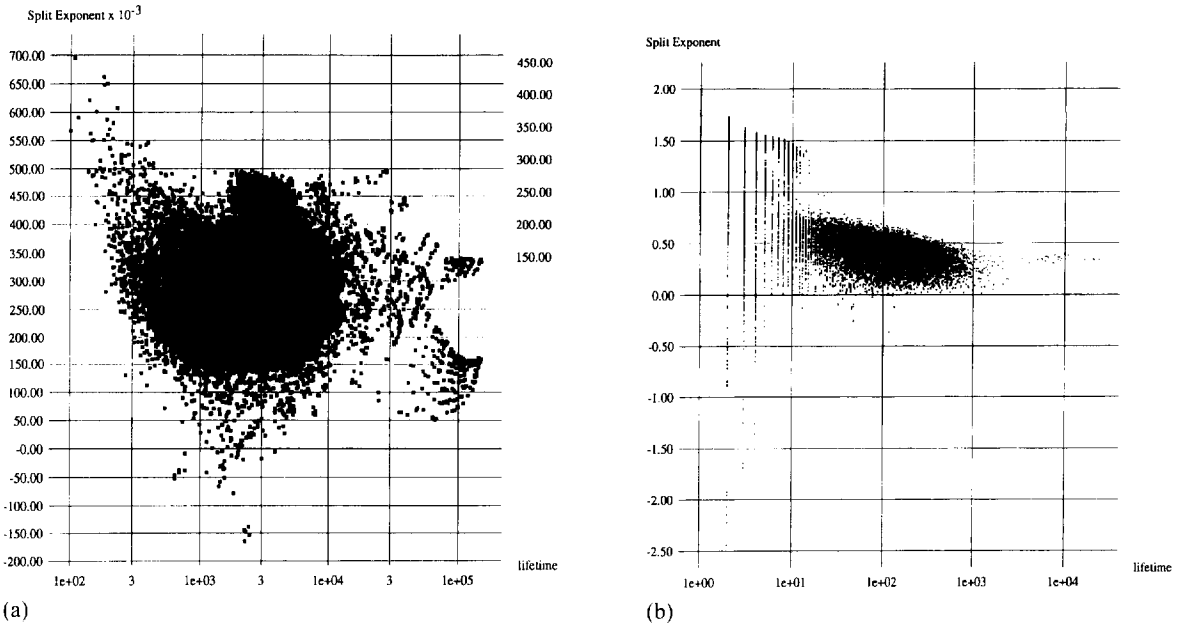

Fig. 7. Split exponent $\lambda_{spl}(i; T_{birth}, T_{division})$ over the lifecycle plotted versus the lifetime of cells. $K = 3.3$, $s = 0.1$, $T_g = 10$, and $T_d = 0$ (a) for cells that divide successfully after their lifecycle, and (b) for cells that die after their lifecycle.

clustering of elements into different groups, a sort of time sharing system is constructed. Thus resources are effectively used, because there is some ordering of the elements. In the partially ordered phase, the "roles" of the elements are also differentiated. As will be discussed in Section 4, cells in large coherent clusters stop dividing but remain existing without dying, while other elements' oscillations are unstable and proceeding to grow faster. For larger K, elements are completely desynchronized, and no ordering for the use of resources is possible. In this case effective use of resources is once again impossible.

Before discussing the detailed dynamics of the system, let us briefly mention the dependence of our dynamical behavior on T_g and T_d. First, the essentially same behavior is observed for $T_d = 0$, independent of T_g. The three phases are found with an increase of K. The dynamics of $x_n(i)$ and the number of cells are basically the same as we have discussed above.

Second, when T_d is negative, cells can grow indefinitely in number, according to our simulation results so far. This is because in our system, s is constantly supplied, and cell's number can increase with the rate $s/(NT_g)$ on the average as long as the death condition is not satisfied. When T_d is negative, the death condition is not satisfied if K is small, where the growth seems to continue indefinitely. The growth rate is slightly enhanced as the desynchronization is increased, up to $K \approx 3.5$, where cell death starts to set in and limits the growth. [2]

4. Growth with differentiation of roles

Here we study the dynamic origin of the sudden change from a steady regime with a small number of cells to the explosive growth in the number, seen at the partially ordered phase as in Fig. 2(c). As an example, let us consider the case given in Fig. 8. Around time steps 4×10^5–6×10^5, the number of cells increases

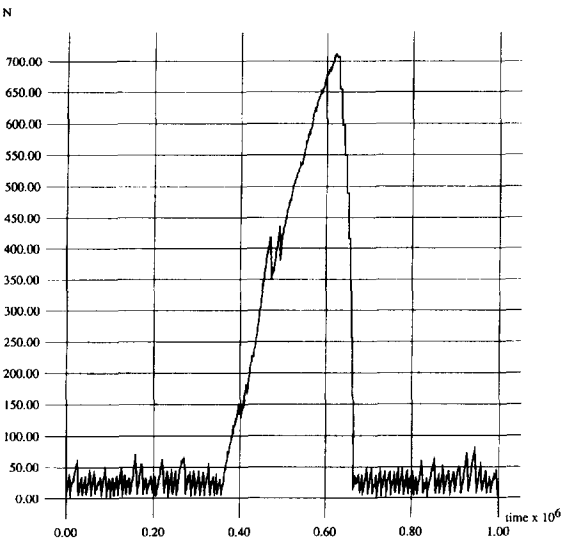

Fig. 8. Temporal evolution of the number of cells N, plotted per 10^3 steps. $K = 3.3$, $s = 0.1$, $T_g = 10$, and $T_d = 0$.

to a large value. This regime is clearly distinct from other regimes. As seen previously in Fig. 2(c), such growth regimes appear intermittently.

In Fig. 9, the split exponents of divided (Fig. 9(a)) and dead (Fig. 9(b)) cells are shown versus time, while the cluster sizes of divided and dead cells are plotted in Fig. 10. Here the cluster size of a cell is defined as the number of cells which have an identical fractional part of $x_n(i)$ up to the given resolution. One can see clearly that the nature of divided and dead cells in this temporal regime, as characterized by λ_{spl}, is different from that in the other regime. From these results and the direct measurement of the time series of $x_n(i)$, the growth regime is characterized as follows:

(i) Cells split into two groups. One group of cells forms a large cluster (typically on the order of $\frac{1}{2}N$), while the other cells are mostly desynchronized with each other, although they can form a synchronized cluster of a smaller size and collapse intermittently.

(ii) The former group of cells neither divides nor dies. In this temporal regime, only groups of cells that are desynchronized with each other divide and lead to growth in the total number of cells. This desynchronization of divided or dead cells

[2] At $T_g = 1$, however, there is an explosive growth for $K \approx 3.5$, where some deaths of cells effectively enhance others' growth, since removal of negative $x(i)$ by death adds up the source term. This is an artifact in our model, since the conservation of the source term is not satisfied when a cell dies.

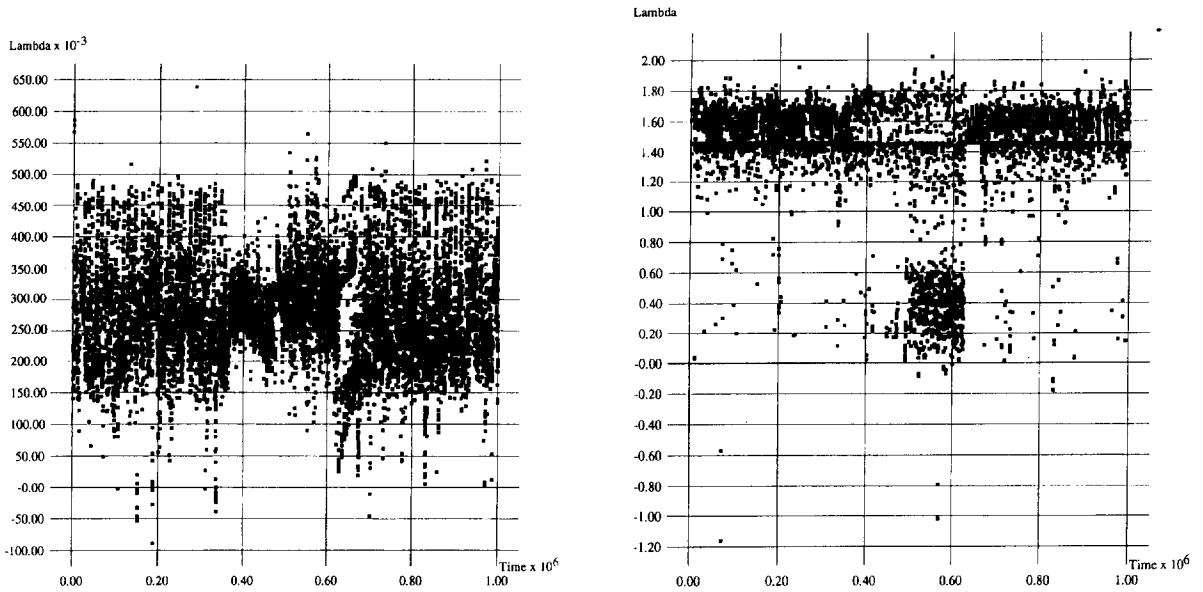

Fig. 9. Split exponent $\lambda_{\mathrm{spl}}(i)$, T_{birth}, T_{division} over the lifecycle for divided (a) and dead (b) cells, plotted in the time course per 10^3 steps. The data are obtained from the simulations for Fig. 8.

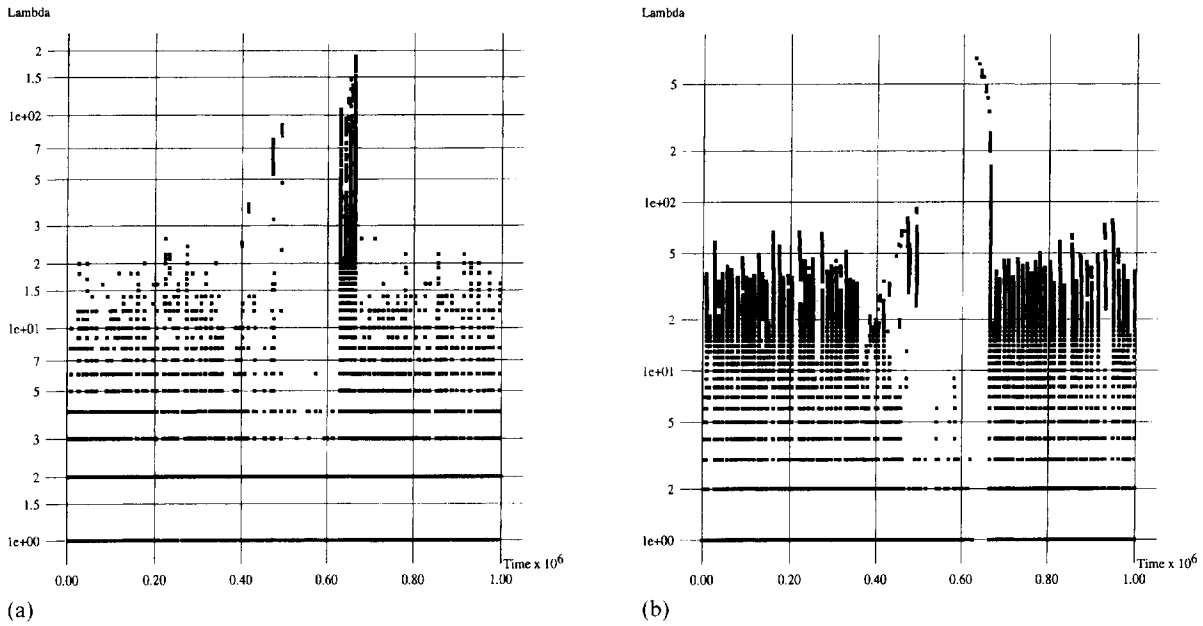

Fig. 10. Cluster number of (a) divided and (b) dead cells, plotted in the time course per 10^3 steps. The data are obtained from the simulations for Fig. 8.

is clearly seen in the time series of their cluster sizes. For example, as Fig. 10 shows, there is a remarkable lack of clusters larger than size 10 around the time steps 5×10^5–6×10^5. In Fig. 9, cells with large and small split exponents are lost during that regime, which corresponds to the fact that the elements in the synchronized cluster are no longer dividing.

(iii) The collapse of the growth occurs because of the synchronous division of many cells belonging to the large cluster. It is clearly seen in Fig. 10 that cells belonging to the cluster divide and die successively at around the 6.2×10^5 time step. We have also measured the time between divisions for each cell (i.e., cell lifetime). This time fluctuates around 1×10^3–10×10^3 for most time steps, but around time step 6.2×10^5, it suddenly jumps to 20×10^3–300×10^3, meaning that the cells that did not divide during the growth regime have successively divided. With this division and the subsequent simultaneous deaths of many cells, the number of cells is drastically reduced back to the normal level.

It is rather interesting to note that the formation of two distinct regimes (i.e., sudden growth and normal growth) is supported by the emergence of the two distinct groups of cells. The group of cells forming the large cluster is necessary to support the growth of the other group which consists of desynchronized cells. The growth of the latter group, on the other hand, suppresses the growth of the former and maintains the stability of this cell society with its inhomogeneous clustering. The differentiation of the roles that the two groups play in producing growth of new cells and maintaining the stability of the system makes possible the growth regime.

Following this separation of roles, it is interesting to draw a cell lineage diagram. In Fig. 11, we have plotted this diagram, where the division process with time is represented by a horizontal line between mother and daughter cells, while a line is terminated when the corresponding cell dies. The diagram shows the differentiation of cells as to the number of offspring, as well as the successive appearance of multiple simultaneous deaths.

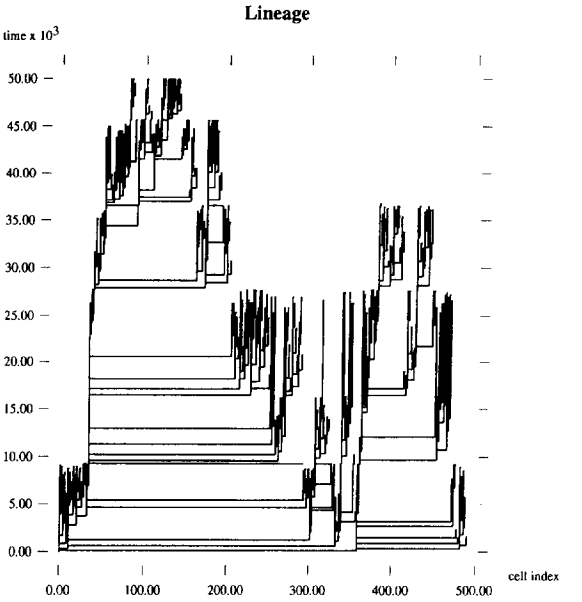

Fig. 11. Cell lineage diagram corresponding to the simulation in Fig.8. The vertical axis shows the time, while the horizontal axis shows a cell index. (For the practical purpose of keeping track of the branching tree, we define the index for the lineage as follows: when a daughter cell j is born from a cell i's kth division, the value $s_j = s_i + 2^{-k}$ is attached to cell j from the mother cell's s_i. The index for cell j is defined in the increasing order of s_j; i.e., the index is sorted so that s_j increases in the order of j. Note that the index for the lineage diagram is different from index i, given just as the order of birth). In the diagram, a horizontal line shows the division of the cell of a smaller index producing the cell of a larger index, while a vertical line is drawn as long as the cell exists (until it dies out).

5. Differentiation of internal states in coupled circle maps

5.1. Multi-phase model

In the model in the previous sections, the internal dynamics was represented by only a single phase dynamics. Since the single circle map has one variable and one attractor for most parameter regimes, the different dynamic behaviors appear only through clustering relationships with other cells. Indeed the different behaviors of a cell are governed by the size of the cluster it belongs to, rather than by its internal states. Thus it is necessary to study a model with internal

variables rather than a single phase variable, in order to study the fixed differentiation memorized in the internal states of a cell.

The author and Yomo have studied a model with biochemical reaction dynamics [9–11], given by a set of ordinary differential equations with switching-like oscillatory dynamics. There the amplitude of the oscillation of chemical concentrations in a cell is essential to the fixed differentiation coded in an internal state of a cell.

Here we consider briefly a simpler model with several phase variables within each cell. Assume that the internal dynamics is composed of several cyclic processes, which are each represented by a circle map. The internal dynamics, given through the interaction among the cyclic processes, is just represented by a coupled circle map:

$$x_{n+1}^m(i) = x_n^m(i) + f(x_n^m(i)) + \sum_l a^{l,m} g(x_n^m(i) - x_n^l(i)) + S_n^m, \quad (4)$$

$$S_n^m = \frac{s^m - \sum_j f(x_n^m(j))}{N}. \quad (5)$$

for $m = 0, 1, 2, \ldots, M$. This superfix m corresponds, for example, to each metabolic chemical cycle involved in each cell, or generally speaking, to some internal process. Here we call this superfix m a *chemical species* for simplicity.

We choose the source term $s^0 > 0$, and $s^m = 0$ for $m > 0$, assuming that the component 0 is the source chemical (e.g., nutrition), while the other components' cycles correspond to the metabolic processes that bring about the growth of the cell. Taking these allocations into account, we define the condition to grow and divide by $\sum_{m=1}^M \mathrm{Int}(x_n^m(i)) > T_g$ while the death condition is defined by $\mathrm{Int}(x_n^0(i)) < T_d$, where $\mathrm{Int}(z)$ denotes the integer part of z. When a cell divides, a new cell is created with chemical species concentration $x_n^m(i) - \mathrm{Int}(x_n^m(i)) - \delta^m$, where δ^m is a small random number (taken from a uniform distribution over $[-10^{-5}, 10^{-5}]$), while the original cell has chemical concentrations $x_n^m(i) - \mathrm{Int}(x_n^m(i)) + \delta^m$.[3]

The coupling terms $a^{l,m}$ and the function g represent the interaction between the cyclic processes. Taking into account the periodic nature of these processes, we adopt again sine circle maps $f(x) = (K/2\pi)\sin(2\pi x)$ and $g(x) = (c/2\pi)\sin(2\pi x)$ to model them. Since the coupling term represents the flow of chemical process, it is postulated that $a^{l,m} = -a^{m,l}$. First we assume that $a^{0,m} = c$ to assure the flow from the source chemical to other species. Next, for other coupling coefficients $a^{l,m}$ we set most of them to zero, but leave a few of them at a constant c. Such pairs (l, m) that give $a^{l,m} \neq 0$ are randomly chosen with the rate L per chemical species. In the present section we take $M = 8$, and $L = 2$. In other words, we have chosen a model with sparse connections. We have made several simulations for this particular coupling sequences of the $a^{l,m}$ with this particular L, M condition.

5.2. Differentiation in chemical compositions

For most parameter regimes, no growth in the number of cells is observed. We have found that either all cells die out or cells stop increasing at a small number (e.g., from 2 to 8). This is because no flow from the source x^0 to the other variables is formed, and thus the growth condition $\sum_{m=1}^M \mathrm{Int}(x_n^m(i)) > T_g$ is not satisfied. When division stops, chemical oscillations of an individual cell are synchronized across all cells. Hence, time sharing for resources is not attained, and further growth is suppressed.

Only at $0.59 \leq c \leq 0.62$ and $0.8 \leq K \leq 1.1$, we have found successive growth and death processes. Here we survey the dynamics in this region.

First we note that all chemical oscillations are desynchronized from cell to cell as the number of cells increases. This desynchronization appears at a rather early stage (after one or two divisions). The temporal average of chemicals starts to differ later, after a few divisions. Here again, clustering is essential for steady growth; otherwise no growth is observed as in most other parameter regimes.

[3] Here we have not divided the fractional part of $x_n^m(i)$ into two, in contrast with the model in Section 3. Indeed the choice is rather arbitrary. Qualitatively identical results are obtained even if half of $x_n^m(i) - \mathrm{Int}(x_n^m(i))$ is transmitted at the division.

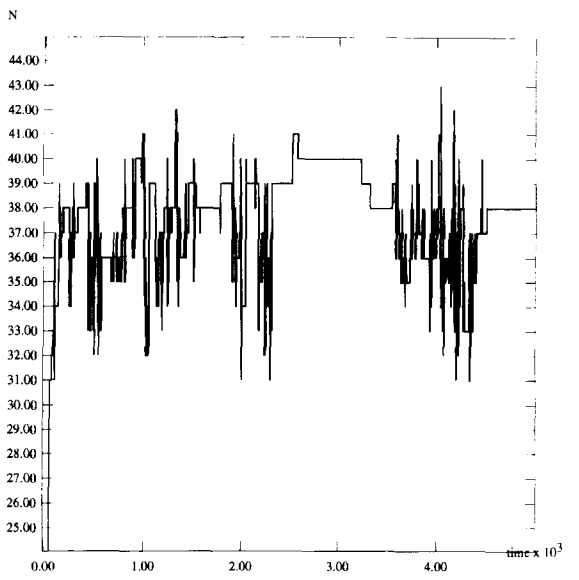

Fig. 12. Temporal evolution of the number of cells N for the coupled circle map of model (4). For Figs. 12–15, we use the parameters $K = 1.1$, $c = 0.59$, $s = 0.8$, $T_g = 1000$, and $T_d = -10$. Simulations are carried out over 5×10^7 steps, starting from a single cell initial condition. The number of cells is plotted per 10^4 steps. In the simulations, we have adopted $a^{l,m} = c$ for the pairs (1,5), (1,8), (2,5), (2,7), (3,1), (3,6), (4,1), (4,2), (5,7), (5,8), (6,2), (6,4), (7,3), (7,4), (8,3), (8,6) with $a^{m,l} = -a^{l,m}$, while other couplings are left to be zero. The same behavior, though, is observed for most other couplings satisfying with $L = 2$.

An example of the time series of the number of cells is given in Fig. 12. In the figure, there are clearly two distinct types of temporal regions; those with and those without a frequent change in the number of cells. In Fig. 12, the latter regime is seen, e.g., around 3×10^7 and 5×10^7 steps. Such multiple temporal regions are typically observed at the parameter region near the boundary for growth (such as $c \approx 0.59$ or $K \approx 1.1$), while regimes without the growth do not contain clearly separated regions (for example at $c = 0.6$ and $K = 1$).

To see the average property of a cell, we define

$$R_n^m(i) = \mathrm{Int}(x_n^m(i))/(n - T_b), \tag{6}$$

where T_b is the time of the latest division (or birth) of the cell. In other words, $R_n^m(i)$ measures the average rotation of the chemical cycle m at the cell i, per step. The rotation $R_{T_d}^m(i)$ at the next division time step T_d gives the rotation rate over the lifecycle of the cell. This rotation $R_n^m(i)$ gives the contribution of each chemical species to the process of division. This quantity gives a measure for the activity of each chemical cycle, or roughly speaking, each chemical composition.

In Fig. 13 we have plotted $R_n^m(i)$ for several time steps n ((a)–(d)), against the cell index, while the rotation $R_{T_d}^m(i)$ at the division is plotted against time in Fig.14. On the average, the M chemical species split into two groups, one for $R_n^m(i) > 0$ (which has two species in the figure), and the other for $R_n^m(i) < 0$ or slightly positive (which has the other six). In other words, the chemical species become differentiated within each cell.

The above "chemical" differentiation applies for each cell. Besides this intra-differentiation, cells are separated into several groups as well, as shown in Fig. 13. In Fig. 13(a), the rotation $R^m(i)$ for each m does not differ by cells so much. As for the average chemical compositions, all cells are almost identical, although the phase of oscillations itself is not synchronized. With time, cells with differently behaving $R^m(i)$ appear as in Fig. 13(b). Roughly speaking, there are two types. In one type, the difference of rotations between two chemical groups (with two and six components, respectively) is much larger; for this type of cell, positive values of $R_n^m(i)$ for two chemicals are much larger than the other type, and the negative values for the other six chemicals are smaller. In the other type of cell, the difference between the rotations of two groups of chemicals is much smaller. Often the sign of $R_n^m(i)$ is opposite, that is, six chemical species have slightly positive $R_n^m(i)$, and the other two have slightly negative ones.

We note that to satisfy the division condition, the sum of $R_n^m(i)$ over chemicals m must exceed the threshold. Thus the above two types correspond to two strategies to satisfy the threshold condition: one is to have few chemical species of large positive rotation values, while the other is to keep the magnitude of negative rotation values smaller. The former cell is chemically specialized, while the latter cell sustains chemical diversity, in the sense that all chemical

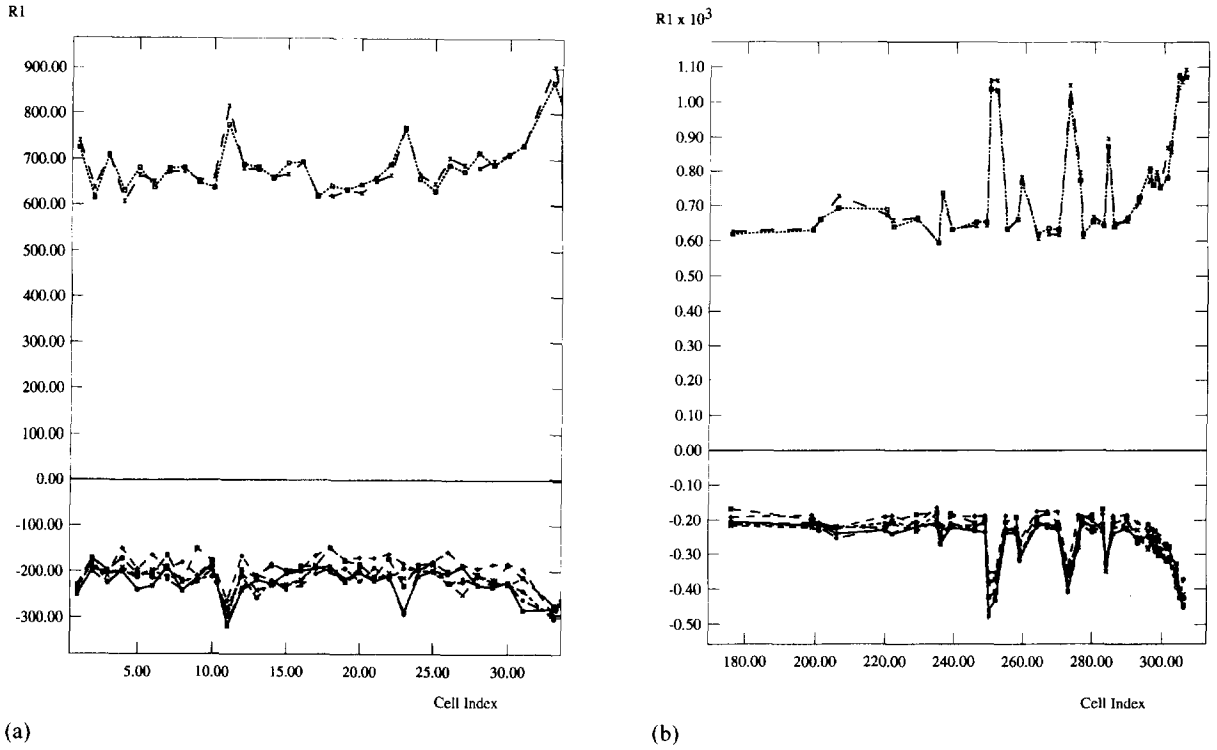

Fig. 13. Continued

cycles contribute to the growth. Differentiation of cell types is associated with that of chemicals contributing to the growth. With this differentiation, the cells' competition for the chemicals is reduced, which is relevant to the growth.

This differentiation is not a snapshot property (i.e., depending on the phase of oscillation), but the average property over a cell's lifecycle.

With a cell's division, the average rotation $R_n^m(i) > 0$ may switch its sign. Indeed the rotation $R_n^m(i) > 0$ oscillates with time n through the division. Hence the types of a cell may change with division. To see if the differentiated type of a cell is recursively transmitted, we have plotted the return map of $R_{T_d}^m(i)$ versus $R_{T_d}^m(j)$ for the cell i born from the cell j by division. If complete recursivity held, the plot would lie on a diagonal line. Starting from a randomly chosen initial condition, there is an approach to recursive transition, but it is attained very poorly. The memory is not preserved as in the model in Section 3.

The rotation $R^m(i)$ stays only within some finite range. In Fig. 14, a majority of cells are recursive around -2×10^{-3} to 1×10^{-3}, while cells deviated from this region are less recursive. Some of the deviated cells around 0.5×10^{-3} to 1×10^{-3} remain there, but most of them lose this characteristic at their next division. As in Fig. 14, there is no point along the diagonal region for highly deviated cells, which means that such deviation is only a one-generation property not transmitted to daughter cells.

5.3. Temporal switch of stages

In Figs. 12 and 13, we have seen that there are two distinct temporal regimes as to the growth patterns. In Fig. 15, we have plotted the rotation $R_{T_d}^1(i) < 0$ (over a cell's lifecycle) versus its time of division, to see the difference between the regimes. There, a larger fraction of cells has $R_{T_d}^1(i) < 0$, while cells with the

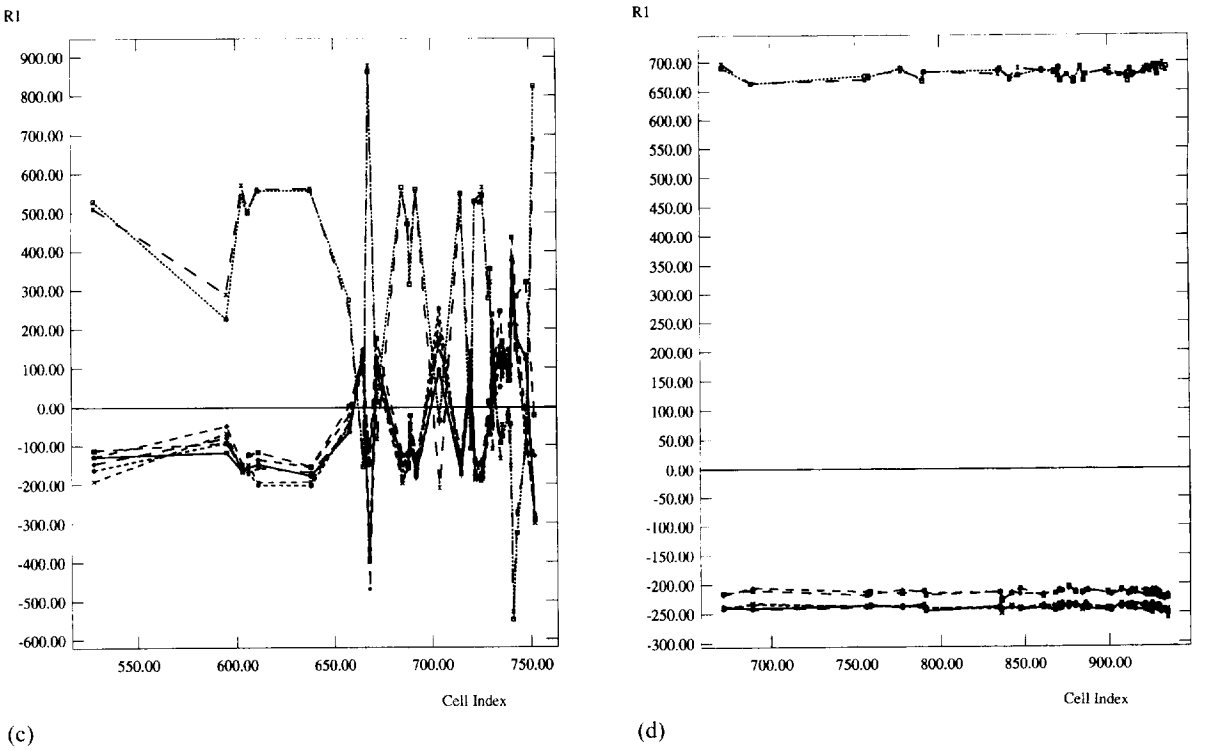

Fig. 13. Rotation $R_n^m(i)$ plotted against the cell index i. The value with a mark gives $R_n^{(m)}(i)$ for $m = 1, 2, \ldots, 8$, for the cell with the index i. Each line connecting between $R_n^{(m)}(i)$ is plotted only for the sake of visualization (i.e., to see the distinction by chemical m clearly). Here cells that do not have marks at the corresponding i are already dead at the time. (When cell i dies, no cell with the index i exists any more. The cell index is attributed in the order of birth, without compressing the indices for dead cells.) For example, cells with the indices 179,180,..., 198 have died at (b). Two lines with $R_n^m(i) > 0$ correspond to the chemical species $m = 4$ and $m = 6$. (a) Time step $n = 10^6$, when the cell number $N = 33$, with the dead cell of the index 32. (b) Time step $n = 8 \times 10^6$. (c) Time step $n = 20 \times 10^6$. (d) Time step $n = 30 \times 10^6$.

opposite rotation appear with a smaller rate. It should be noted that Figs. 12 and 13 suggest that the birth of cells is more frequent when the value $R_n^m(i)$ is scattered by cell i. If the distribution of $R_{T_d}^m(i)$ over cell i is concentrated, division is suppressed. For example, around time step 3×10^7, a single type of cell dominates as in Fig. 13(c). That is, $R_n^m(i)$ for all m takes almost all the same values for cell i. Around this time step, growth is inhibited, as is seen in Fig. 12 (see also Fig. 15). As in Figs. 13(d) and 15, growth is sustained by the heterogeneity of the cell society.

We have also measured the histogram of $R_n^m(i)$ over all cells for some time intervals. The distribution has two broad-band peaks during the time course when cells are dividing frequently, although more than $\frac{3}{4}$ of the cells are accumulated in one peak (at $R^1(i) < 0$). Cell division stops when the distribution has one (broad) peak. The coexistence of different types of cells seems to be necessary for the overall growth of cells.

Summarizing several simulations, the cell society evolves as follows: As cell types get similar (e.g., with the same sign of $R_n^m(i)$ for all species m), cell division is suppressed. A homogeneous cell society, however, is unstable, and the cells' small differences start to be amplified. A few cells start to be differentiated (i.e., to have a different sign of $R_n^m(i)$) when growth is enhanced. Then cells divide several times, followed by some cell deaths. Successive changes between a rather homogeneous cell society, and a highly heterogeneous

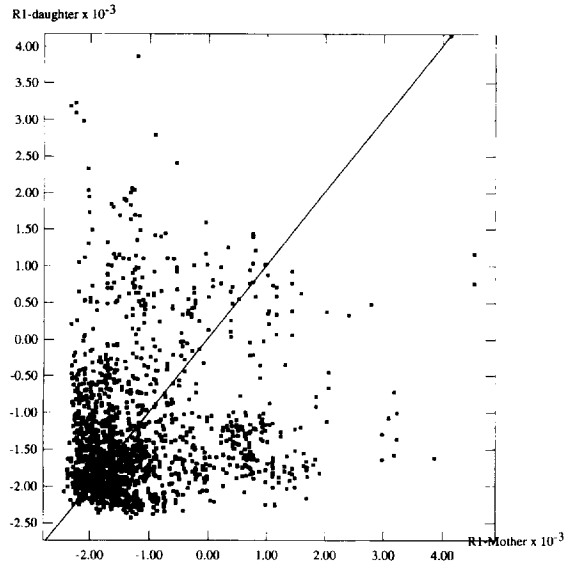

Fig. 14. Return map of the average rotation $R^1_{T_d}(i)$ over the lifecycle. A daughter cell's average rotation over the lifecycle is plotted versus its mother's cell's average before the division to the daughter.

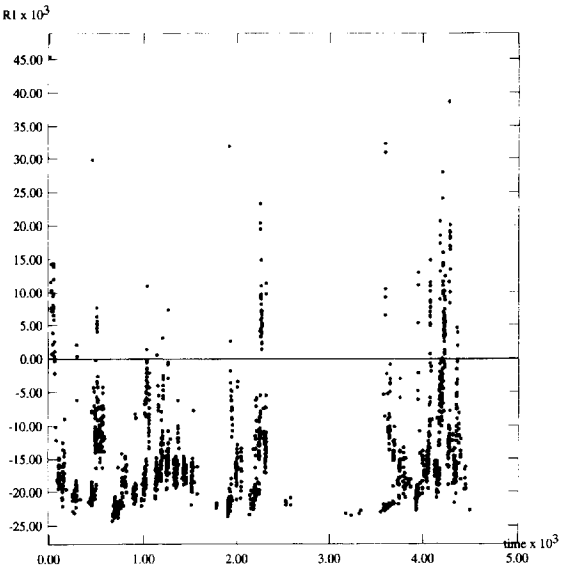

Fig. 15. Rotation $R^1_{T_d}(i)$ over a lifecycle. When a cell is divided its average rotation over the lifecycle is plotted at the corresponding time step of the division.

society allowing for growth are observed repeatedly. It should be noted that the differentiation of different cell types is not just by their phase of oscillation, but by the change of chemical species contributing to the condition $R^m_n(i)$.

6. Discussion

In the present paper, we have studied a simple coupled map model inspired by cell biology. In a biological system, there always exists an intrinsic tendency toward diversity and individuality. A biological system is essentially heterogeneous, as is simply seen in the fact that no two cells are identical, in contrast with physical particles like electrons which are all exactly the same [22]. In terms of dynamical systems, this diversification is purported to be supported by the orbital instability of the evolution of a cellular state provided by a chaotic system [19,20]. As is seen in the clustering phenomena in coupled map systems, elements split into groups with different dynamical behaviors. Assuming such instability exists at the individual cell level, an important question is how macroscopic robustness is sustained.

Our hypothesis here is that the stability is sustained at an ensemble level. Coupled nonlinear systems have a rich variety of collective dynamics, ranging from low- to high-dimensional behavior [16,17,23,24] (see also [25] for collective behavior of locally coupled dynamical systems). Furthermore this collective dynamics often maintains stability even if it is high-dimensional chaos.

In the present simulations, it should be noted that a system keeps partial synchronization to sustain the growth in the number of elements. When growth is possible, the system bounces between synchronization and complete desynchronization. When synchronization dominates, multiple simultaneous deaths of cells occur, and the system restores diversification having different oscillatory dynamics. When desynchronization dominates, on the other hand, no cooperative use of resources is possible. There is too much competition for resources, and cells die before increasing their number. The relevance of partial synchronization is clearly seen in the growth regime, where the

differentiation into a small group of rapidly dividing cells and a majority group of non-diving cells makes possible the overall growth of cells. In the regime where cells are able to grow, the split exponent is slightly positive.

In a model with an internal coupled circle map, a few types of cells are formed with different internal phase rotations. This variety, to some degree, is necessary for growth; when it is lost the speed of cell divisions is lowered, until diversity is recovered after the increase of cell number due to division which changes the nature of the chemical dynamics in each cell.

Summing up, the macroscopic stability of the growing state is sustained by partial synchronization supplied by a change in the number of degrees of freedom (i.e., number of cells). With this partial synchronization, the chaotic instability of the whole chemical dynamics is kept rather weak although many degrees of freedom are involved. In an unrelated ecological model, the author and Ikegami have proposed the notion of "homeochaos" [18] which is stability at the macroscopic level supported by high-dimensional weak chaos, where chaotic itinerancy [12,26,27] over several clustered states is found. It should be noted that the triplet structure there – "weak chaos", "partial synchronization", "many degrees of freedom" – necessary for stability is common to our model. The main difference here is the mechanism that sustains the partial synchronization. In our model here, it is due to the change in the degrees of freedom, while in the model of [18], it is sustained through the change of mutation rates.[4]

There remains an important question from our standpoint, that is, how the recursive transmission of cell type is attained in a dynamical system approach. Since we have demonstrated the tendency of cells to become more diversified, the origin of faithful self-replication is a non-trivial question. Our hypothesis here is that the "digitalization" of states through clustering, and the choice of initial conditions leads to recursive transmission. A cell with a given differentiated behavior transmits its character through its initial condition. In the simulations in Section 5, a cell's character is not well transmitted to its daughter cell, but some extension of the intra–inter dynamics may lead to the recursive transmission of a mother cell's characteristics to its daughters. Indeed, in the recent model of the author and Yomo [9], such recursivity is partially accomplished. In that model, each internal dynamics has degrees of freedom not only for the phase but also for the amplitude. The internal dynamics, by itself, can show an on–off type switching oscillation, which may be relevant to producing recursivity, since a state is easily coded digitally with the switching-type oscillation.

In short, our dynamical systems viewpoint of biology is summarized as follows:

(1) Heterogeneity by isologous diversification $\Leftrightarrow$ clustering due to orbital instability in each internal dynamics.
(2) Macroscopic robustness $\Leftrightarrow$ collective dynamics of coupled nonlinear elements, in particular homeochaos.
(3) Recursivity $\Leftrightarrow$ choice of initial conditions with digitalization of differentiated states.

Although our model is much too simplified, it provides a starting point for the study of biology from the above standpoint of dynamical systems theory. Besides the dynamic origin of a cell differentiation, our results suggest the relevance of heterogeneity to the growth of the cell society. The differentiation of roles upon division reminds us of germ line segregation, while multiple simultaneous deaths occurring repeatedly, reminds us of apoptosis. In this context, our result supports the view that cellular interaction is relevant to the apoptosis observed in multicellular organisms.

The temporal oscillation of the population of different types of cells in Section 5 may provide a basis for the understanding of the experiment by Ko et al. [28], where *E. coli* successively cultivated in a well-stirred liquid culture differentiate into distinct types whose populations show a complex oscillation in the time course.

[4] Although the number of variables itself does not change in the model of [18], the effective degrees of freedom changes with the mutation rate, since the populations of many "species", whose number changes with the mutation rate, vanish in the model. Thus the correspondence with the present model may be even stronger than the statements above.

Interaction-dependent differentiation of cell types is also found in tumor formation, as shown in a series of experiments by Rubin [29]. In the experiments, the cell-to-cell interaction is not global in contrast with the experiment by Ko et al. Since we have not included any spatially local effects, our results cannot be directly applied to their experiment. In general, spatially local interactions among cells are, of course, important as development proceeds in a multicellular organism. Indeed we have made some simulations of a "short-ranged-coupling" version of our model. So far the scenario presented in the paper is still valid there. First, the clustering of the phase of oscillations supports the time sharing for resources, and then at a later stage, cells located closely to each other start to be differentiated following the scenario in the present paper. At the next stage, due to the local interaction, differentiated cells start to become organized spatially, leading to the pattern formation. Simultaneous death of cells appears again but in a spatially localized manner.

To model the developmental process further, introduction of cellular motions in real space will also be required. Cells with internal dynamics move in real space according to their interaction with surrounding elements. Such a model leads to a novel class of dynamical systems, called a coupled map gas and is discussed in [30].

As dynamical systems, the present study casts two novel classes of models. One is a dual coupled map, and the other is open chaos.

Dual coupled map: In the model of Section 5, the dynamics can be regarded as a dual coupled map, in the sense that each variable $x_n^m(i)$ on a two-dimensional lattice (m, i) is coupled over two spaces, i.e., over all cells i and over chemical species m. Both the couplings are global, although the former is all-to-all, and the latter is sparsely connected. Since each globally coupled map shows clustering, the dual coupled map leads to a competition of clustering with respect to each space (cell and chemical). We have made several simulations for two-dimensional dual coupled maps with all-to-all global interactions for each dimension [31]. With the increase of nonlinearity, first the selection of clustering in one direction (while retaining the synchronization against the other space) appears. Then elements lose synchronization against both directions, where the clustering involves both the dimensions, and is coded by a combination of the two spaces. In the present context of a cell society, this combined clustering leads to the differentiation of cells with different chemical characters (roles).

Open Chaos: Our system, as a whole, has some kind of orbital instability analogous with chaos. Within the internal dynamics, an orbit is expanded with the mechanism of chaos, and then is divided. Although this expansion–division process looks like a Baker's transformation, there is a clear difference. After cell division, the dimension of the phase space (i.e., the number of degrees of freedom) is increased, while in a Baker's transformation the orbit stays in the original phase space. We have coined the term "open chaos" [20] to address such a chaotic instability which is inseparable from the change of the phase space itself.

Due to the change of the number of degrees of freedom, most quantifiers for dynamical systems are not applicable, since they require stationarity of the phase space. In the present paper we have adopted the split exponent to characterize the amplification rate of differences in the internal states of two cells. Since the exponent is defined locally at each time, it is an effective measure in open ended dynamical systems.

In a model allowing for the growth of the number of elements, we have found that the effective time sharing of system resources is formed due to the presence of partially clustered states. A balance between synchronization and desynchronization is necessary here, for the effective use of resources, which enables the growth of the number of cells (agents). The sharing of resources by the clustering here may be applied to economics, where a breakdown of the time sharing system by synchronization may correspond to an economic crash.

Acknowledgements

I am grateful to Tetsuya Yomo and Takashi Ikegami for stimulating discussions, and to Brant Hinrichs for critical reading of the manuscript. The work is

partially supported by Grant-in-Aids for Scientific Research from the Ministry of Education, Science, and Culture of Japan.

References

[1] K. Kaneko, Progr. Theoret. Phys. 72 (1984) 480; Physica D 34 (1989) 1; Simulating physics with coupled map lattices, in: Formation, Dynamics, and Statistics of Patterns, eds. K. Kawasaki, A. Onuki and M. Suzuki (World Scientific, Singapore, 1990); Collapse of Tori and Genesis of Chaos in Dissipative Systems (World Scientific, Singapore, 1986, based on thesis of 1983).
[2] K. Kaneko, ed., Theory and Applications of Coupled Map Lattices (Wiley, New York, 1993); Special Issue on CML, Chaos 2 (3) (1992).
[3] B. Goodwin, Temporal Organization in Cells (Academic Press, London, 1963).
[4] J. Tyson, B. Novak, G.M. Odell, K. Chen and C.D. Thron, Trends Biochem. Systems 21 (1996) 89.
[5] S.A. Kauffman, The Origin of Order (Oxford University Press, Oxford, 1993).
[6] A.M. Turing, Proc. Roy. Soc. London B 237 (1952) 641.
[7] L. Glass and S.A. Kauffman, J. Theoret. Biol. 34 (1972) 219.
[8] F.A. Bignone, J. Theoret. Biol. 161 (1993) 231.
[9] K. Kaneko and T. Yomo, Isologous diversification: A theory of cell differentiation, Bull. Mat. Biology 59 (1997) 139.
[10] K. Kaneko and T. Yomo, Physica D 75 (1994) 89.
[11] K. Kaneko and T. Yomo, A theory of differentiation with dynamic clustering, in: Advances in Artificial Life, eds. E. Moran et al., Vol. 329 (Springer, Berlin, 1995).
[12] K. Kaneko, Phys. Rev. Lett. 63 (1989) 219; Physica D 41 (1990) 137.
[13] K. Kaneko, Physica D 54 (1991) 5.
[14] K. Okuda, Physica D 63 (1993) 424.
[15] D. Dominguez and H.A. Cerdeira, Phys. Rev. Lett. 71 (1993) 3359.
[16] N. Nakagawa and Y. Kuramoto, Progr. Theoret. Phys. 89 (1993) 313; Physica D 75 (1994) 74; V. Hakim and W.J. Rappel, Phys. Rev. A 46 (1992) 7347.
[17] K. Kaneko, Phys. Rev. Lett. 65 (1990) 1391; Physica D 55 (1992) 368; Physica D 86 (1995) 158.
[18] K. Kaneko and T. Ikegami, Physica D 56 (1992) 406; T. Ikegami and K. Kaneko, Chaos 2 (1992) 397.
[19] K. Kaneko, Artificial Life 1 (1994) 163–177.
[20] K. Kaneko, Physica D 75 (1994) 55–73.
[21] K. Kaneko, Physica D 77 (1994) 456.
[22] W.M. Elsasser, Proc. Nat. Acad. Sci. 81 (1984) 5126.
[23] A.S. Pikovsky and J. Kurths, Phys. Rev. Lett. 72 (1994) 1644.
[24] G. Perez et al., Physica D 63 (1993) 341; S. Sinha et al., Phys Rev. A 46 (1992) 6242.
[25] H. Chaté and P. Manneville, Progr. Theoret. Phys. 87 (1992) 1.
[26] I. Tsuda, in: Neurocomputers and Attention, eds. A.V. Holden and V.I. Kryukov (Manchester University Press, Manchester, 1990); World Futures 32 (1991) 167; Neural Networks 5 (1992) 313.
[27] K. Ikeda, K. Matsumoto and K. Ohtsuka, Progr. Theoret. Phys. Suppl. 99 (1989) 295.
[28] E. Ko, T. Yomo and I. Urabe, Physica D 75 (1994) 84.
[29] A. Yao and H. Rubin, Proc. Nat. Acad. Sci. 91 (1994) 7712; M. Chow, A. Yao and H. Rubin, ibid 91 (1994) 599; H. Rubin, ibid 91 (1994) 1039; 91 (1994) 6619.
[30] T. Shibata and K. Kaneko, Coupled Map Gas, in preparation.
[31] K. Kaneko, unpublished.
[32] E. Mjolsness, D.H. Sharp and J. Reinitz, J. Theoret. Biol. 152 (1991) 429.